Journal of Thermal Analysis and Calorimetry, Vol. 96 (2009) 1, 117–124

MEASUREMENT OF REACTION ENTHALPY DURING PRESSURE OXIDATION OF SULPHIDE MINERALS

I. Bylina[1], *L. Trevani*[2], *S. C. Mojumdar*[1], *P. Tremaine*[2] *and V. G. Papangelakis*[1*]

[1]Department of Chemical Engineering and Applied Chemistry, University of Toronto, 200 College Street, Toronto ON, M5S 3E5, Canada
[2]Chemistry Department, University of Guelph, Guelph, ON, N1G 2W1, Canada

A calorimetric method for determining the enthalpy of the aqueous oxidation of sulfide minerals at high temperatures and oxygen pressures has been developed and evaluated under conditions relevant to industrial pressure oxidation operations. This information is important for heat balance calculation and optimization of the pressure reactor design. Experiments were carried out on a differential scanning calorimeter (DSC) with a commercial mixing cell. Enthalpy measured during oxidative dissolution of pyrite (Valdenegrillos, Spain), pentlandite with pyrrhotite (Sudbury, Ontario, Canada) and impure chalcopyrite (Victoria, Australia) minerals at 150°C and partial oxygen pressures of 3.4 and 5.5 MPa have been performed and found to be consistent with theoretical estimations.

Keywords: *DSC, enthalpy, ICP-AES, mixing cell, oxidation, SEM, sulphide minerals, XRD*

Introduction

Autothermal operation of pressure oxidation processes requires knowledge of the exothermic reactions in hydrometallurgical operations. Consequently, the measurement or calculation of the reaction enthalpy is an important factor in the design of such operations.

Even if enthalpies for mineral oxidative leaching can be estimated from standard thermochemical data [1, 2], these values can only be used as an approximation of the actual process heat requirements, because: (*i*) natural minerals are rarely found as pure crystalline phases, (*ii*) the chemistry of mineral oxidation and dissolution is very complex and several reactions and products occur to a variety of extents, and (*iii*) the observed heat of reaction depends on other factors, such as extent of grinding or activation [1]. Therefore, measured heats of mineral oxidation under process conditions are useful for accurate heat balances, optimization of autoclave design, study and modeling of the hydrometallurgical processes.

We have used a heat flow differential scanning calorimeter (DSC C80) from Setaram designed for measurement of heat of mixing and heat of reaction at normal and elevated temperatures and pressures in this work. Although several studies are reported in the literature for measuring heat of mixing [1–4], heat of dissolution of gases in liquids [4, 5], heat of reactions at high temperatures [3], none of these studies have involved the presence of a solid in contact with both, a liquid and a gas phase, simultaneously. Thermal analysis and calorimetry, along with XRD, XRF, ICP-AES and SEM are very useful techniques for materials characterization and identification of chemical reaction [6–22]. In the present study we have employed these techniques in addition to DSC, to investigate the oxidative pressure leaching of three natural sulphide minerals: pyrite (FeS_2), pentlandite with pyrrhotite ($Fe_{4.5}Ni_{4.5}S_8$; FeS), and chalcopyrite ($CuFeS_2$). The selection of FeS_2 was due to its omnipresence in sulphide oxidation processes as an impurity as well as to its relevance in the production of gold. Pyrite can be found in a pure crystalline phase and therefore it is a good reference system. Pentlandite and chalcopyrite are usually found in mixtures and in combination with other minerals such as pyrrhotite and pyrite. Our purpose was to develop a calorimetric experimental method to measure the heat of oxidative leaching of sulphide minerals which usually involves temperatures ranging from 150 to 230°C, and partial oxygen pressures from 0.3 to 1.4 MPa.

Experimental

The enthalpies of oxidative leaching of sulfide minerals were measured using a differential scanning calorimeter (DSC C80, Setaram) equipped with a commercial mixing cell able to operate at temperatures up to 300°C and pressures up to ~21 MPa. The cell with a nominal volume of 9.1 cm^3 was made

* Author for correspondence: vladimiros.papangelakis@utoronto.ca

1388–6150/$20.00
© 2009 Akadémiai Kiadó, Budapest
Akadémiai Kiadó, Budapest, Hungary
Springer, Dordrecht, The Netherlands

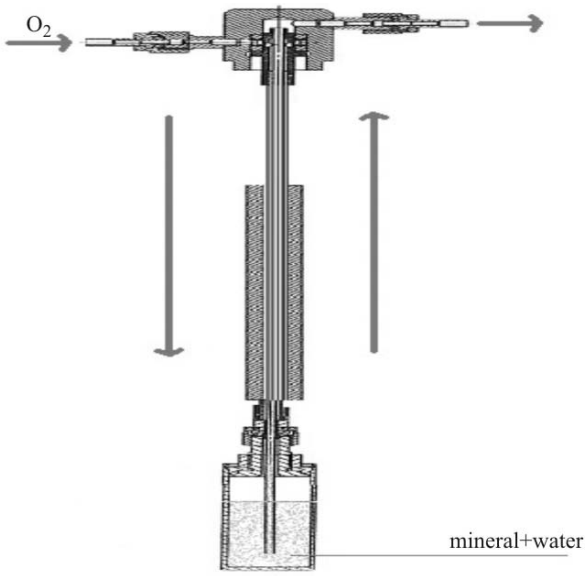

Fig. 1 Schematic diagram of the mixing cell

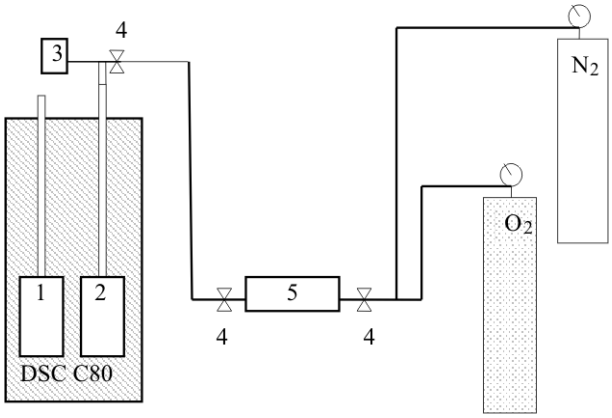

Fig. 2 Experimental calorimeter setup: 1 – reference and 2 – experimental cells (C80 Setaram differential scanning calorimeter); 3 – pressure transducer; 4 – three-way high pressure valves and 5 – flow meter

from stainless steel and used in combination with a glass liner (4 cm^3 volume) to prevent degradation of the stainless steel cell when working with corrosive mixtures at high temperatures. A schematic diagram of the cell and its inlet and outlet tubes used for gas injection is shown in Fig. 1. A schematic diagram of the experimental setup, calorimeter and injection system is presented in Fig. 2.

Mineral characterization

Natural sulphide minerals, pentlandite with pyrrhotite (Sudbury, Ontario, Canada), pyrite (Valdenegrillos, Spain) and chalcopyrite (Victoria, Australia) were purchased from Excalibur Mineral Corp. (USA).

The chemical analysis of the mineral samples was determined using Inductively Coupled Plasma-Atomic Emission Spectrometry (ICP-AES) on a Perkin Elmer Optima 3000 DV instrument. In addition, elemental analysis was determined using X-ray Fluorescence (XRF) on a Philips 2404 sequential X-ray Fluorescence equipment, which was calibrated with the appropriate sulfide standards. The phases present in each mineral sample were identified using powder X-ray diffraction (XRD) on a Philips PW1830 powder X-ray Diffractometer. The searchable International Center of Diffraction Data (ICDD), 2005 database was used for identification of the phases in the mineral samples.

XRD analysis showed that pyrite crystals were pure, consisting of only one phase (detection limit ~5–3 mass%). On the other hand, pentlandite was found to contain pyrrhotite; chalcopyrite to consist of four major phases. Based on the XRD pattern and XRF analysis, the chalcopyrite sample consisted of 50.30 mass% chalcopyrite ($CuFeS_2$), 25.44% siderite ($FeCO_3$), 13.50% pyrite (FeS_2), 9.35% quartz (SiO_2) and minor amount of MgO and Al_2O_3. The above three mineral samples also contained trace metals as determined by ICP-AES analysis. Ni and Ca were found in pyrite; Cu, Co and Mg in pentlandite; Ni, Mg and Ca in chalcopyrite. The results of ICP-AES and XRF analysis are summarized in Table 1.

The morphology and purity of pyrite, pentlandite and chalcopyrite were investigated using a Scanning

Table 1 Sulphide minerals characterization using ICP-AES and XRF analysis

Sulphide mineral	Source	Chemical analysis/mass%*	Mineralogy/mass%
Pyrite crystals	Valdenegrillos, Spain	47.11 Fe 49.90 S	95 FeS_2* 5 Fe_2O_3
Pentlandite with Pyrrhotite	Sudbury, Ontario, Canada	48.19 Fe 14.06 Ni 32.07 S	41.11 $Fe_{4.5}Ni_{4.5}S_8$* 52.77 FeS 6.12 trace metals
Chalcopyrite	Victoria, Australia	34.97 Fe 17.42 Cu 22.41 S	50.30 $CuFeS_2$** 25.44 $FeCO_3$ 13.50 FeS_2 9.35 SiO_2

*ICP-AES analysis, **XRF analysis

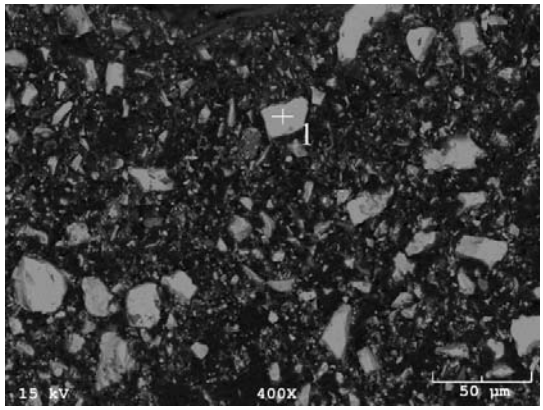

Fig. 3 SEM image of the surface of a polished specimen of pyrite (particle size <37 μm), 400×, 1 – Pyrite

Electron Microscope (SEM) with digital imaging capabilities (fraction <37 μm) by means of Secondary Electrons (SE) and Backscattered Electrons (BSE). The SEM was a JEOL, JSM-840, complemented by a PGT/AAT EDS detector (thin window) and an IXRF 500 digital pulse processor, allowing for X-ray microanalysis and digital imaging via SE, BSE and X-ray signals.

The SEM examination shown in Fig. 3 confirmed that the pyrite sample is pure. A similar examination also showed that our pentlandite and chalcopyrite samples had variable compositions. Figure 4 shows pentlandite with pyrrhotite and pyrite in minor amounts. Significant variability in composition was also observed in the chalcopyrite sample as seen in Fig. 5.

Chemical analysis of minerals, filtrates and residues

The chemical composition of minerals, solid residues and filtrates was determined by ICP-AES. Mineral samples of 50.0±0.1 mg were digested in 25 mL of boiling aqua regia with continuous agitation for

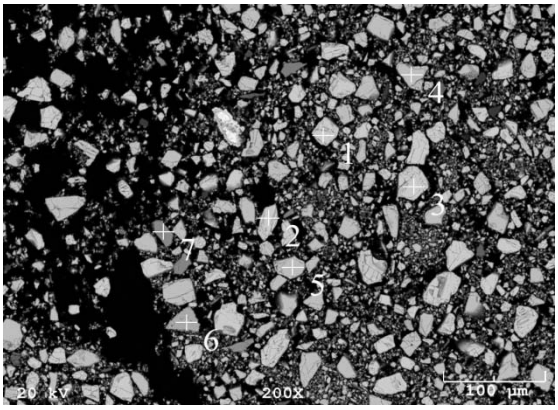

Fig. 4 SEM image of the surface of a polished specimen of pentlandite with pyrrhotite sample (particle size <37 μm), 200×, 1–3: pentlandite $Fe_{4.5}Ni_{4.5}S_8$, 4, 5: pyrrhotite FeS, 6, 7: pyrite FeS_2

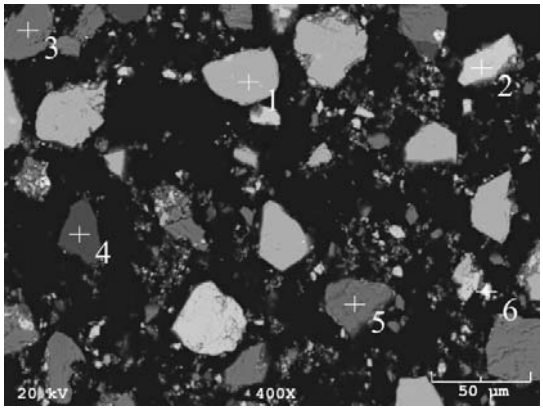

Fig. 5 SEM image of the surface of a polished specimen of chalcopyrite sample (particle size <37 μm). 400×, 1 – FeS_2; 2 – $CuFeS_2$; 3 – Fe_2O_3; 4 – SiO_2; 5 – Fe_2SiO_4, $Fe(AlO_2)_2$; 6 – NiS, NiSb

approximately 2 to 3 h. The resulting solution was then filtered and diluted with deionized water to 250 mL.

At the end of the calorimetric measurement, the experimental cell and its contents were cooled down. All unreacted solids remained in contact with the solution for at least 4 h, before being separated at room temperature. After determining the solution pH with a pH-indicator strip (EMD Chemicals Inc., Germany), the slurry was filtered with Fisherbrand filter paper P2. The filtrate was separated and stored and the cell with any remaining residue was rinsed with 5% HNO_3. The residues were dried in an oven at 100°C for 1–2 h and cooled down in desiccators. The dried residues were weighed and digested in boiling aqua regia (25 mL) before they were analyzed by ICP-AES.

Experimental procedure

The mineral oxidation was carried out under isothermal conditions. The cell with a weighed amount of mineral (0.0300 to 0.0600±0.0002 g) and deionized (Millipore Milli-Q Water System) water (2.0000±0.0002 g) was placed into the calorimeter chamber at room temperature. To expel air from the cell, nitrogen gas was passed through the cell for 20 min at a flow rate of 20.39±0.13 sccm, and then the outlet valve of the cell was closed. The mineral and water were then kept under nitrogen atmosphere at a pressure of 1.4 MPa while heating the cell at a heating rate of 2°C min^{-1} to the final temperature of 150°C and final pressure of ~2.1 MPa. It took approximately 3 to 4 h to reach a stable temperature.

Once the temperature was stable to ±0.02°C, oxygen was injected into the cell at a constant flow rate of 10.62 (±1.13%) up to a partial oxygen pressure of 3.4 or 5.5 MPa depending on the experiment. Subse-

quently, the inlet valve of the cell was closed and the system was kept at 150°C for 10 h since preliminary experiments showed that in some cases up to 8–9 h were required to complete the reaction. After that, the DSC system was cooled down to room temperature with a built-in fan at a rate of 2°C min^{-1}. Cooling was completed in about 4 h. The prolonged period of cooling may cause additional oxidation of the minerals, albeit at progressively slower rates as the temperature drops.

The nitrogen and oxygen flow rates were measured with a Brooks 5850E series controller that was previously calibrated with a portable calibrator Bios Definer 220 (±2.2%). The pressure was measured with a pressure-sensitive transducer Gefran rated to 35 MPa.

The performance of the DSC was first evaluated by measuring the enthalpy of dissolution of potassium chloride salt (Standard Reference Material 1655, the National Institute of Standards and Technology) in water at 25°C using a specially designed teflon container [23–25]. The measured enthalpy of dissolution of KCl, 17.25±0.01 kJ mol^{-1} (±0.06%) was found to be in excellent agreement with the literature value of 17.22 kJ mol^{-1} [26].

Mineral powders were ground in air by a ring mill for about 1 min, and dry-sieved to several size fractions. The mineral fraction with a particle size smaller than 37 μm was used for the heat of reaction measurements.

Experimental enthalpy corrections

The overall enthalpy change, ΔH_{exp}, was obtained by integration of the DSC curve as a function of time. The measured enthalpy includes: (*i*) the heat of oxidation-dissolution of the mineral, ΔH_{oxid} (mineral); (*ii*) the heat of dissolution of oxygen in water, ΔH_{diss} (O_2); (*iii*) and the heat required for raising the oxygen temperature from room to 150°C, ΔH_{heat} (O_2). The following equation describes the relationship.

$$\Delta H_{exp}=\Delta H_{oxid}\text{ (mineral)}+\Delta H_{diss}(O_2)+\Delta H_{heat}(O_2) \quad (1)$$

To determine the contributions of the ΔH_{diss} (O_2) and ΔH_{heat} (O_2) to the overall experimental enthalpy, blank experiments were carried out. The $\Delta H_{blank}=\Delta H_{diss}(O_2)+\Delta H_{heat}(O_2)$ was obtained from a run with water and oxygen, but without mineral, under the same conditions adopted for the experiments. The heat of mineral oxidation was then estimated using Eq. (2). The Setsoft 2000 software distributed by Setaram was used for this estimation.

$$\Delta H_{oxid}\text{ (mineral)}=\Delta H_{exp}-\Delta H_{blank} \quad (2)$$

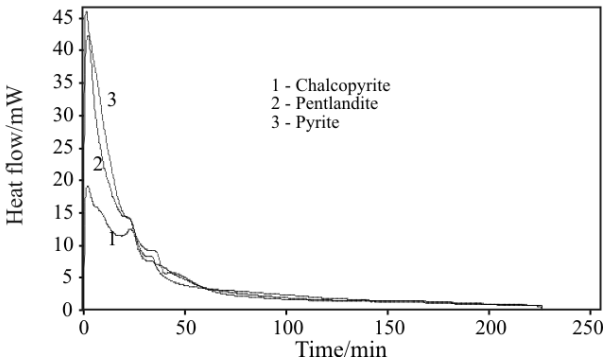

Fig. 6 DSC curves for oxidation of 1 – chalcopyrite, 2 – pentlandite and 3 – pyrite samples at 150°C and partial oxygen pressure 3.4 MPa

Results and discussion

Typical DSC curves for pyrite, chalcopyrite and pentlandite samples are presented in Fig. 6. The main reactions are presented in Table 2 (Eqs (4)–(12)). The theoretical heats of reaction for our mineral assemblages at 150°C were estimated from the standard molar enthalpies of formation of the reactants and products in these idealized reactions. The calculations were done with the HSC Chemistry 5.0 software. The heat of formation of pentlandite was taken from Cemic and Kleppa [27] since the compound was not in the HSC database.

Heat of pyrite oxidative pressure leaching

The amount of unreacted pyrite in the solid residue must be known to determine the molar heat of reaction. However, the very small reactor volume made the recovery of the samples very difficult and some approximations had to be made in order to estimate the degree of conversion from mineral to products.

Effect of mineral mass at constant oxygen pressure

Because the pyrite specimen was pure, the analysis of the measurements was simpler than for pentlandite and chalcopyrite. The XRD analysis of the residue after pyrite oxidation showed significant amount of unreacted pyrite. The XRD patterns of the original mineral and the solid products were identical. The amount of unreacted pyrite in the solid residue was estimated from the sulphur content in the residue after digestion using Eq. (3) and the moles of hematite formed – using Eq. (4).

$$\text{mol } (FeS_2)_{\text{un-reacted}}=\text{mol } S_{residue}/2 \quad (3)$$

$$\text{mol } Fe_2O_3=[\text{mol } Fe_{residue}-(\text{mol } S_{residue}/2)]/2 \quad (4)$$

Table 2 Theoretical enthalpy of sulphide mineral oxidation at 150°C

Reaction	Theoretical reaction enthalpy/kJ (HSC v. 5, [27])
Chalcopyrite	
1) $CuFeS_2+4H^++O_2(g)=Cu^{2+}+Fe^{2+}+2S^0+2H_2O$	–401.62
2) $CuFeS_2+4O_2(g)=Cu^{2+}+Fe^{2+}+2SO_4^{2-}$	–1750
3) $2Fe^{2+}+0.5O_2+2H^+=2Fe^{3+}+H_2O$	–207.34
Pyrite	
4) $2FeS_2+4H^++O_2(g)=2Fe^{2+}+4S^0+2H_2O$	–405.08
5) $FeS_2+3.5O_2(g)+H_2O(l)=Fe^{2+}+2SO_4^{2-}+2H^+$	–1551
6) $2Fe^{2+}+0.5O_2+2H^+=2Fe^{3+}+H_2O$	–207.34
Pentlandite	
7) $(FeNi)_{4.5}S_8+4H^++O_2(g)=4.5Ni^{2+}+4.5Fe^{2+}+8S^0+2H_2O$	–387.0
8) $(FeNi)_{4.5}S_8+16O_2(g)=4.5Ni^{2+}+4.5Fe^{2+}+8SO_4^{2-}$	–7478.5
9) $2Fe^{2+}+0.5O_2+2H^+=2Fe^{3+}+H_2O$	–207.34
Pyrrhotite	
10) $FeS+2H^++0.5O_2(g)=Fe^{2+}+S^0+H_2O$	–278.64
11) $FeS+2O_2(g)=Fe^{2+}+SO_4^{2-}$	–952.74
12) $2Fe^{2+}+0.5O_2+2H^+=2Fe^{3+}+H_2O$	–207.34

Table 3 Enthalpy of pyrite oxidation at 150°C and P_{O_2}=3.4 and 5.5* MPa

Mineral/mg	Reacted FeS_2/			Net heat of reaction/J	Molar heat of reaction/ kJ mol^{-1}	Specific heat of reaction/ kJ kg^{-1}
	mg	%	mol 10^{-4}			
39.9	21.0	53	1.75	–52.6	–301	–2505
50.0	26.1	52	2.18	–60.9	–284	–2369
60.2	26.7	44	2.23	–59.2	–266	–2216
ΔH_{av}= –284±14 kJ mol^{-1} (–2363±118 kJ kg^{-1})						
60.0*	26.1	43	2.18	–65.0	–299	–2489
60.2*	26.7	44	2.23	–61.0	–274	–2282
ΔH_{av}= – 287±13 kJ mol^{-1} (–2386±104 kJ kg^{-1})						

Table 3 summarizes the results and presents the enthalpy values for pyrite oxidation. The average specific enthalpy value at P_{O_2}=3.4 MPa is ΔH_{av}= –2363±118 kJ kg^{-1}. The degree of reacted pyrite decreases from 53 to 44% with increasing mineral mass from 0.04 to 0.06 g (Table 3).

Because of the small amount of the samples, filtrates and residues the ratio of sulfate to elemental sulphur formed and the ratio of ferrous to ferric irons were not determined. This analysis would have enabled us to know the exact nature of chemical reactions occurring between FeS_2 and O_2. Furthermore, the theoretical enthalpies of sulphur conversion from pyrite to elemental sulphur and to sulfate are markedly different (Table 2, reactions 4 and 5). Interestingly, the heat of pyrite conversion to elemental sulphur is of the same order of magnitude as Fe(II) oxidation to Fe(III): reactions 4 and 6 in Table 2.

If we assume that all sulphur from pyrite is oxidized to sulfate and all iron oxidized to Fe(III), the heat of the overall reaction would be –1655 kJ mol^{-1} FeS_2. In this case, the estimated enthalpy (–1655 kJ mol^{-1}) is 5.8 times higher than the average experimental value of –284±14 kJ mol^{-1} at P_{O_2} of 3.4 MPa (Table 3). However, if we assume that all sulphur from pyrite is converted to elemental sulphur and all iron oxidizes to Fe(III), then the overall heat of reaction would be –306 kJ mol^{-1} FeS_2. This value is close to the experimental enthalpy –284±14 kJ mol^{-1} at a partial oxygen pressure of 3.4 MPa (Table 3), suggesting that pyrite oxidation under these conditions proceeded to elemental sulphur. The fact that the reaction did not proceed to completion is likely because of O_2 transfer limitations.

Effect of oxygen partial pressure in pyrite oxidation

The observation that the higher the mineral weighting in the reactor the lower the fraction of mineral reacted (Table 3) is also consistent with the postulation for O_2 transfer limitation caused by the lack of stirring. Stirring the mixture would have increased the mass transfer between solids and dissolved oxygen. Under the present experimental conditions, oxygen flows into the cell (and therefore providing some stirring) only for 21 min at P_{O_2} of 3.4 MPa, which is not enough to complete the mineral dissolution. Under industrial conditions the time required for 98% Ni extraction from a sulfide flotation concentrate in oxidative pressure leaching with sulfuric acid at 150°C is about 30 min [28]. Under neutral conditions with less dissolved Fe(III) in solution, this time is expected to be longer.

Pyrite was also oxidized under a higher partial oxygen pressure value of 5.5 MPa (Table 3). Under this pressure, oxygen required longer time (29 min) to fill up the cell. However, the increase of oxygen pressure did not oxidize the mineral further. The amount of reacted pyrite remained was almost the same, 43 *vs*. 44% (Table 3). This is consistent with Williamson and Rimstidt [29] who reported that pyrite oxidation is not much affected by the concentration of dissolved oxygen in water. The average experimental enthalpy value under P_{O_2} =5.5 MPa is –287±13 kJ mol^{-1} (Table 3) was also close to the theoretical enthalpy estimated based on the assumption that sulphide sulphur is oxidized to elemental sulphur.

Heat of pentlandite sample

The pentlandite sample was a mixture of ~41.11% pentlandite and ~52.77% pyrrhotite (Table 1), and therefore, the heat of pressure oxidation will be the result of the oxidation of both components. Consequently, we evaluated the contribution of each component to the total heat released. We estimated the extent of pentlandite leaching by assuming that all reacted nickel remains in solution due to the high acidity of the solution, pH 1 to 2 [30]. We further assumed that any nickel in the solid residue was unreacted pentlandite ($Fe_{4.5}Ni_{4.5}S_8$) which amount was estimated by Eq. (5). The amount of unreacted pyrrhotite was then estimated by Eq. (6):

$$\text{mol } (Fe_{4.5}Ni_{4.5}S_8)=\text{mol } Ni_{residue}/4.5 \quad (5)$$

$$\text{mol (FeS)}=\text{mass (FeS)}/M(\text{FeS})= [\text{mass of dry residue}–\text{mol } (Fe_{4.5}Ni_{4.5}S_8)\cdot M(Fe_{4.5}Ni_{4.5}S_8)]/M(\text{FeS}) \quad (6)$$

where mol($Fe_{4.5}Ni_{4.5}S_8$) and mol(FeS) are the moles of unreacted pentlandite and pyrrhotite, respectively; M($Fe_{4.5}Ni_{4.5}S_8$) and M(FeS) are the molar masses of pentlandite and pyrrhotite, respectively.

The experimental enthalpies of the pentlandite sample are summarized in Table 4. The average enthalpy at P_{O_2} of 3.4 MPa (Table 4) is ΔH_{av}= –3102±151 kJ kg^{-1} of reacted sample.

Similarly to pyrite, the theoretical enthalpies of pentlandite and pyrrhotite conversion to elemental sulphur (Table 2, reactions 7 and 10) are much lower than for sulfate formation (reactions 8 and 11). If we assume that all sulphide sulphur is converted to elemental sulphur and take into account the heat of oxidation of Fe(II) to Fe(III) – reactions 7 and 9 in Table 2, then the enthalpy of pentlandite oxidation would be –854 kJ mole^{-1} pentlandite (–1106 kJ kg^{-1}); whereas for pyrrhotite oxidation would be –382 kJ mole^{-1} pyrrhotite (–4349 kJ kg^{-1}). Because the pentlandite sample is composed of two minerals, the composite ΔH value for oxidation of 1 kg of such mixture would be –2930 kJ kg^{-1}. This value is in good agreement with our experimental measurements of –3102±154 kJ kg^{-1} at P_{O_2} of 3.4 MPa (Table 4).

Effect of oxygen partial pressure on pentlandite sample

In the case of oxidation under increased partial oxygen pressure, the reacted pentlandite increased from 56 to 79% and, at the same time, pyrrhotite was reduced from 42 to 17% (Table 4). Under higher oxy-

Table 4 Enthalpy of oxidation of pentlandite $Fe_{4.5}Ni_{4.5}S_8$ (41.11%) with pyrrhotite FeS (52.77%) sample at 150°C and P_{O_2}=3.4 and 5.5* MPa

Total mineral/ mg	$Fe_{4.5}Ni_{4.5}S_8$; FeS/mg	Reacted $Fe_{4.5}Ni_{4.5}S_8$/mg; %	Reacted FeS/ mg; %	Net heat of reaction/J	Specific heat of reaction/kJ kg^{-1}
29.9	12.3; 15.8	7.0; 56	5.6; 35	–37.1	–2951
30.3	12.5; 16.0	7.1; 57	6.7; 42	–44.7	–3252
		ΔH_{av}= –3102±151 kJ kg^{-1}			
30.3*	12.5; 16.0	9.8; 79	2.8; 17	–64.9	–5130
30.0*	12.3; 15.8	9.0; 73	2.6; 17	–65.8	–5642
		ΔH_{av}= –5386±256 kJ kg^{-1}			

Table 5 Enthalpy of oxidation of chalcopyrite sample (50.30% $CuFeS_2$) at 150°C and P_{O_2}=3.4 and 5.5* MPa

Total mineral/mg	$CuFeS_2$/mg	Residue (reacted)/ mg	Reacted $CuFeS_2$/mg; %	Net heat of reaction/J	Specific heat of reaction/kJ kg^{-1}
31.0	15.59	13.8 (17.2)	11.19; 72	–25.2	–2251
40.1	20.17	27.0 (13.1)	12.52; 62	–30.2	–2413
50.2	25.25	38.0 (12.2)	11.80; 47	–29.0	–2457
60.2	30.28	44.7 (15.5)	11.72; 39	–29.2	–2490
		ΔH_{av}= –2328±119 kJ kg^{-1}			
49.9*	25.10	26.6 (23.3)	16.0; 53	–50.4	–3149
50.0*	25.15	26.8 (23.2)	16.02; 53	–48.0	–2996
		ΔH_{av}= –3073±77 kJ kg^{-1}			

gen pressure the pentlandite oxidation is favored over pyrrhotite. These results suggest that further pentlandite oxidation occurs at higher oxygen concentration, or that a galvanic effect is in place between pentlandite and pyrrhotite which is facilitated at higher O_2 pressure resulting in accelerated dissolution of pentlandite.

Heat of chalcopyrite sample oxidation

The chalcopyrite sample used in this study was a mixture of four major minerals, and the measured heats of pressure oxidation were the result of the oxidation and dissolution of all components. For consistency, we report here the heat of reaction in per kg of reacted mineral, even though, chalcopyrite ($CuFeS_2$) is 50.30% of the total sample mass.

The pH of the final solution was around 2 and all copper in the residue was accounted as copper from unreacted chalcopyrite [30–32]. The measured enthalpies of chalcopyrite mineral leaching are summarized in Table 5. The average enthalpy of chalcopyrite oxidation at P_{O_2} of 3.4 MPa is –2328±119 kJ kg^{-1} of reacted chalcopyrite. The percentage of reacted chalcopyrite reduces with the mineral mass. This tendency was also observed for pyrite and pentlandite oxidation (Tables 3 and 4) and has again been attributed to the lack of stirring.

If we assume that all sulphur from chalcopyrite is converted to elemental sulphur and all Fe(II) is converted to Fe(III), the estimated enthalpy of pressure oxidation is –505 kJ mol^{-1} (–2753 kJ kg^{-1}) $CuFeS_2$. This calculation is taking into account the amounts of chalcopyrite (50.30%), siderite (25.44%) and pyrite (13.50%) in the chalcopyrite sample.

Effect of oxygen pressure on chalcopyrite oxidation

Under increased partial oxygen pressure at constant mineral mass (50 mg), the amount of reacted chalcopyrite increased slightly from 47 to 53% (Table 5), indicating that oxygen concentration is not significantly affecting the chalcopyrite surface oxidation. A similar observation was made previously for pyrite oxidation. This behaviour is consistent with the oxidation mechanism reported by Hackl *et al.* [33]. According to Hackl *et al.* [33], the oxidative pressure leaching of chalcopyrite is stifled by molten sulphur, which wets and agglomerates the sulphide particles and prevents further oxidation at temperatures higher than the melting point of sulphur, 120–160°C. High copper recovery can be obtained if the temperature is raised to 200°C or higher [33].

Conclusions

A calorimetric method for determining the reaction enthalpy of sulfide mineral oxidation at high temperatures and high oxygen pressures has been developed and evaluated under conditions relevant to industrial pressure oxidation operations. The heat of oxidative pressure leaching of sulphide minerals is important for the heat balance and optimization of the autoclave design.

The reliability of the developed method has been tested first by measuring the enthalpy for the pyrite mineral oxidation. The theoretical enthalpy for pyrite oxidation at 150°C, estimated based on the assumption that sulphide sulphur converted to elemental sulphur, is –306 kJ mol^{-1}. This value is vey close to the experimental enthalpy at P_{O_2} of 3.4 and 5.5 MPa: –284±14 and –287±13 kJ mol^{-1}, respectively.

All measured enthalpies for natural sulphide mineral oxidation at 150°C showed good reproducibility with a standard deviation of about 5%.

The measured enthalpies are consistent with their oxidation mechanisms as reported in the literature. It was shown that the concentration of dissolved oxygen in water is important factor in the leaching of pentlandite mineral but not so for pyrite, or chalcopyrite. This is consistent with passivation mechanisms by molten S encapsulation as shown in the literature.

Acknowledgements

This work has been financially supported by Natural Science and Engineering Research Council (NSERC) and Vale Inco. The acquiring and interpreting of the XRD, XRF and SEM analysis results, provided by George Kretschmann and Dr. Gorton from the Geology Department at the University of Toronto are gratefully acknowledged.

References

1 Z. Xiao, Q. Chen, Z. Yin, H. Hu and P. Zhang, Thermochim. Acta, 416 (2004) 5.
2 W. Y. Gao, Y. W. Wang, L. M. Dong and Z. W. Yu, J. Therm. Anal. Cal., 85 (2006) 785.
3 P. N. Aukett and J. Bensted, J. Thermal Anal., 38 (1992) 701.
4 C. Mathonat, V. Hypek, V. Majer and J-P. E. Grolier, J. Solution Chem., 23 (1994).
5 D. Koschel, J.-Y. Coxam and V. Majer, Ind. Eng. Chem. Res., 46 (2007) 1421.
6 F. A. Lopez, M. C. Ramirez, J. A. Pons, A. Lopez-Delgado and F. J. Alguacil, J. Therm. Anal. Cal., 94 (2008) 517.
7 J.-F. Masson and S. Bundalo-Perc, J. Therm. Anal. Cal., 90 (2007) 639.
8 B. Chowdhury and S. C. Mojumdar, J. Therm. Anal. Cal., 81 (2005) 179.
9 P. Simon, E. Illekova and S. C. Mojumdar, J. Therm. Anal. Cal., 83 (2006) 67.
10 S. C. Mojumdar, M. Sain, R. Prasad, L. Sun and J. E. S. Venart, J. Therm. Anal. Cal., 90 (2007) 653.
11 S. Jingyan, L. Yuwen, L. Jie, W. Zhiyong and W. Cunxin, J. Therm. Anal. Cal., 90 (2007) 761.
12 L'. Krajči, I. Janotka, I. Kraus and P. Jamnicky, CERAMICS-Silikaty, 51 (2007) 217.
13 S. Y. Sawant, V. M. S. Verenkar and S. C. Mojumdar, J. Therm. Anal. Cal., 90 (2007) 669.
14 E. Jona, M. Sapietová, V. Pavlík, G. Rudinská, D. Ondrušová, M. Pajtášová and S. C. Mojumdar, Res. J. Chem. Environ., 11 (2007) 23.
15 V. A. Drebushchak and A. I. Turkin, J. Therm. Anal. Cal., 90 (2007) 795.
16 I. Janotka and L'. Krajči, CERAMICS-Silikaty, 39 (1995) 105.
17 M. Dovál', M. Palou and S. C. Mojumdar, J. Therm. Anal. Cal., 86 (2006) 595.
18 S. C. Mojumdar and L. Raki, J. Therm. Anal. Cal., 85 (2006) 99.
19 G. Vourlias, N. Pistofidis, K. Chrissafis and G. Stergioudis, J. Therm. Anal. Cal., 90 (2007) 769.
20 S. C. Mojumdar, K. Mazanec and M. Drabik, J. Therm. Anal. Cal., 83 (2006) 135.
21 G. Vourlias, N. Pistofidis, E. Pavlidou and K. Chrissafis, J. Therm. Anal. Cal., 90 (2007) 777.
22 S. C. Mojumdar and L. Raki, J. Therm. Anal. Cal., 82 (2005) 89.
23 V. P. Nesterenko, J. Therm. Anal. Cal., 80 (2005) 575.
24 D. G. Archer, J. Phys. Chem. Ref. Data, 28 (1999) 1.
25 Z. H. Zhang, Z. J. Ku, H. R. Li, Y. Liu and S. S. Qu, J. Therm. Anal. Cal., 79 (2005) 169.
26 V. B. Parker, Thermal Properties of Uni-Univalent Electrolytes, Natl. Stand. Ref. Data Series – Natl. Bur. Stand. (U.S.) 2 (1965) in Handbook of Chemistry and Physics, David R. Lide Editor-in-Chief, 79th Ed., 1998–1999, pp. 5–103.
27 L. Cemic and O. J. Kleppa, Phys. Chem. Miner., 14 (1987) 52.
28 D. G. E. Kerfoot, E. Krause, B. J. Love and A. Singhal, Hydrometallurgical process for the recovery of nickel and cobalt values from a sulfidic flotation concentrate, US Patent, Patent US 6,428,604 B1, Aug. 6 (2002).
29 M. A. Williamson and J. D. Rimstidt, Geochim. Cosmochim. Acta, 58 (1994) 5443.
30 D. L. Jones, Process for extraction of metal from an ore or concentrate containing nickel and/or cobalt, US Patent 6171564, Jan. 9 (2001).
31 C. F. Baes and J. R. E. Mesmer, The hydrolysis of cations. John Wiley and Sons, 1986.
32 E. C. Todd, D. M. Sherman and J. A. Purton, Geochim. Cosmochim. Acta, 67 (2003) 2137.
33 R. P. Hackl, D. B. Dreisinger, E. Peters and J. A. King, Hydrometallurgy, 39 (1995) 25.

DOI: 10.1007/s10973-008-9883-4